Theory of light scattering from self-affine surfaces: Relationship between surface morphology and effective medium roughness

Angel Yanguas-Gil,* Brent A. Sperling,† and John R. Abelson‡

Department of Materials Science and Engineering, University of Illinois at Urbana-Champaign, Urbana, Illinois 61801, USA

(Received 1 November 2010; revised manuscript received 21 April 2011; published 18 August 2011)

Using Rayleigh-Rice scattering theory we have studied the influence of surface morphology on the optical response of self-affine surfaces. We have established a mathematical relationship between the surface roughness (d) as determined by spectroscopic ellipsometry (SE) using the effective medium approximation (EMA) and the parameters controlling the morphology of the surface: root-mean-square roughness (w), correlation length (ξ), and roughness (Hurst) exponent (α). These three parameters affect the roughness value measured by ellipsometry. However, when the correlation length is smaller than the wavelength, the dependence is contained in a single parameter $w\delta$ that is proportional to the product of the surface roughness and the local slope $\delta = w/\xi^\alpha$. The fact that the local slope of a surface increases only very slowly during growth explains the linear dependence experimentally found between w as measured by scanning-probe microscopy and the vertical roughness determined by the effective medium approach.

DOI: 10.1103/PhysRevB.84.085402 PACS number(s): 78.20.−e, 78.66.Jg, 78.68.+m, 42.25.Fx

I. INTRODUCTION

The morphology of material surfaces, i.e., roughness, plays a crucial role in a wide variety of optical, electronic, chemical, and mechanical properties. Surface morphology evolves during the vapor-phase deposition or etching of materials. Surfaces tend to roughen because of the random arrival of incident flux as well as shape instabilities caused by curvature-dependent attachment rates, shadowing effects, and other factors.[1–4] Surfaces also tend to smoothen because of surface diffusion or re-emission of adspecies.[1,5,6] The competition between these mechanisms produces the net evolution in roughness, which generally increases with film thickness. The desire to understand and control the morphology has motivated the development of spectroscopic ellipsometry (SE) as a real-time, quantitative probe.[7–14] Ellipsometry data are most often transformed into the optical properties, and the thicknesses of the layers present using Fresnel reflection and transmission coefficients in combination with multilayer models. Surface (and interface) morphology is modeled indirectly using an effective medium approximation (EMA) in which the physical roughness is represented by a flat layer whose optical properties are a volume-weighted average of the two media; for a surface, these are the film material (the hills of roughness) and the ambient (the empty space between the hills).[15,16] In order to model the optical properties of this roughness layer, Bruggeman's model is frequently used. This model assumes that the layer is composed of a random mixture of void and solid material, and that the characteristic size of the homogeneous region is much smaller than the wavelength. Although the model can be written to account for shape anisotropy in the regions, normally the isotropic case is used in the modeling of surface roughness. The morphology is thus reduced to two parameters, the volume fraction of solid material f and the thickness of the EMA layer d_s. As a simplifying heuristic, most researchers set the volume fraction $f = 0.5$ and treat the EMA-roughness layer as a one-parameter fit, the thickness. While there is no fundamental justification for the choice $f = 0.5$, we will present several results using this value to facilitate comparison with the literature.

In contrast, studies using atomic force microscopy (AFM) or other scanning probe methods reveal that actual surface morphologies are very complex, even in the absence of effects such as crystallographic faceting and columnar growth.[17–20] A common statistical measure is the power spectral density (PSD), defined as $S(\mathbf{q}) = \langle \widehat{h}(\mathbf{q},t)\widehat{h}(\mathbf{q},t)^*\rangle$, where $\widehat{h}(\mathbf{q},t)$ is the Fourier transform of heights and $\mathbf{q}$ is the wavenumber in the plane of the surface, i.e., the inverse of the lateral range. As a consequence of Parseval's theorem $\int S(\mathbf{q})d\mathbf{q} = w^2$, where w is the rms surface roughness; this is a value usually reported in the literature. Many thin films examined using AFM exhibit a self-affine characteristic: over a threshold wavenumber $2\pi/\xi$, where ξ is the correlation length, the PSD asymptotically approaches $S(q) = \langle \widehat{h}(\mathbf{q},t)\widehat{h}(\mathbf{q},t)^*\rangle_{|\mathbf{q}|=q} \sim q^{-(2\alpha+2)}$, where α is roughness (Hurst) exponent. Consequently, the morphology of self-affine surfaces must be described using three parameters: the rms roughness w, the correlation length ξ, and the roughness exponent α. In thin-film growth, dynamic-scaling theory suggests links between the values of the roughness exponent and different prevalent growth mechanisms; however, systems whose growth cannot be described by the dynamic-scaling theory often also exhibit the same power dependence on the PSD described above.[1]

Previous authors have correlated the thickness of the EMA roughness layer with the rms roughness detected by AFM.[8,9,12,16,21–26] As noted above, the roughness generally increases during the deposition of thin-film materials as the result of competing mechanisms. Thus, thin-film growth provides an important means to test the effect of surface morphology on the optical response. For example, in the growth of hydrogenated amorphous silicon (a-Si:H) films on smooth substrates, several groups have found a linear relationship between d_s and w, but each reported a different proportionality constant despite the use of comparable measurement conditions in SE and AFM.[8,21,24] We previously explored a modified growth situation: a thin, highly rough a-Si:H layer was deposited onto a flat substrate using intentionally "bad" growth parameters, followed by the growth of a thick film using growth parameters, which normally afford very smooth films.[10] The result was

 ©2011 American Physical Society

striking: SE indicated that the surface became *smoother* upon deposition of the thick film, whereas AFM revealed continuous *roughening*. Thus, the correlation between SE and AFM measurements is not unique but must be a function of morphological details beyond the rms roughness.

This work examines two fundamental questions. First, what is the optical response of a self-affine surface in terms of the three parameters of the PSD? We derive the result using Rayleigh-Rice theory. We show that the solution can be separated into mathematical terms that depend only on the morphology and terms that depend only on the optical constants of the material. Thus, the dependence on morphology is described by a formalism that is independent of the materials system.

Second, in what respects can (or cannot) an EMA, with only a single free parameter, model the characteristics of surface morphology as detected by AFM? We show that a linear relationship between d and w is generally *not* expected. However, in cases that obey dynamic-scaling theory, the surface roughness, correlation length, and the roughness exponent are strongly coupled: when the local surface slope $\delta \sim w/\xi^{\alpha}$ remains constant with time, a linear relationship occurs. Thus, we explain on theoretical grounds the varying experimental results found in the literature. When a linear correlation exists but the slope is different, it must be the case that the surfaces in question have different local slopes; when a departure from linearity occurs, it must be the case that dynamic scaling does not hold, e.g., by the use of discontinuous film-growth conditions.

II. MODEL

Our approach[27] proceeds as follows. First we calculate the optical response of a self-affine surface using scattering theory as a function of the three parameters that are needed to describe the surface morphology. Second we cast that result in terms of the optical function measured by SE. Third we apply the Bruggeman EMA with a volume fraction $f = 0.5$ to calculate the thickness of the roughness layer (later we will discuss the influence of the fraction). Finally we compare the rms roughness of the self-affine surface with the thickness of the EMA layer to determine the functional relationship between them. In all cases we assume that the surface layer sits on top of an optically opaque bulk layer, i.e., we do not complicate the analysis by including the reflection of beams from an underlying interface.

A. Scattering model

In thin-film growth both the vertical extent of surface roughness (as quantified by w) and the lateral extent (as quantified by ξ) are typically much smaller than the wavelength of the incident light λ. These conditions fall within the domain of the Rayleigh-Rice formalism, in which Maxwell's equations are solved considering a series expansion of the electromagnetic fields on the small parameter w/λ. Franta and Ohlídal presented a model for the scattering of light by statistically rough surfaces up to second order using the Rayleigh-Rice formalism.[28] They obtained a closed expression

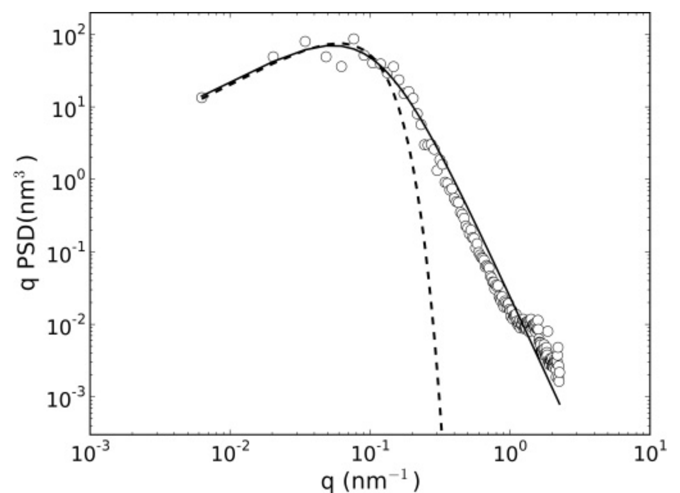

FIG. 1. Comparison of an experimental PSD of a surface determined by AFM, the self-affine (4), and Gaussian parameterizations.

for the change of the reflection Fresnel coefficient attributable to surface roughness given by

$$\Delta r_{p,s} = \int_{-\infty}^{\infty}\int_{-\infty}^{\infty} f_{p,s}(q_x,q_y)S(q_x - n_0k_0\sin\theta_0,q_y)dq_x dq_y \tag{1}$$

where $S(q_x,q_y)$ is the surface PSD and $f_{p,s}(q_x,q_y)$ are two functions that determine the optical response of the system in p and s polarizations. These depend on the optical properties of the two media forming the interface, the wavenumber of the radiation $k_0 = 2\pi/\lambda$, and the angle of incidence θ_0.

The functions $f_{p,s}(q_x,q_y)$ are given by

$$\begin{aligned} f_p(q_x,q_y) = A_p + \{&B_{31p}q^2(b-c) - B_{32p}q_x \\ &+ B_{61p}q_x[q^2(b-c)^2 + (q^2+bc)^2] \\ &+ B_{62p}(b-c)(q_y^2+bc)\}/(q^2+bc) \end{aligned} \tag{2}$$

and

$$f_s(q_x,q_y) = A_s + B_{5s}\frac{(b-c)\left(q_x^2+bc\right)}{q^2+bc} \tag{3}$$

where $b = \sqrt{n_0^2k_0^2 - q^2}$ and $c = \sqrt{n_1^2k_0^2 - q^2}$.

In these expressions n_0 and n_1 are the complex refraction indices of the incident and reflecting medium and the A_i, B_i coefficients depend on the optical properties of the interface materials and the angle of incidence. Their expressions are given in the Appendix.

Franta and Ohlídal applied this model to study the scattering and ellipsometric response of thin films characterized by a Gaussian PSD.[29] However, the assumption of a Gaussian fails to reproduce the PSD measured in most experimental systems, which are self-affine; in particular the Gaussian model significantly underestimates the contribution at high wavenumbers (Fig. 1).

We have chosen a parametrization of the PSD that is able to reproduce the asymptotic behavior characteristic of self-affine surfaces,[30,31]

$$S(q) = \frac{\alpha w^2\xi^2}{\pi}\frac{1}{(1+\xi^2q^2)^{\alpha+1}}, \tag{4}$$

where w, ξ, and α are the rms roughness, correlation length, and the roughness exponent previously defined. We further assume that $S(q) = 0$ over a certain cut-off wavenumber $q > q_c$. This limits the self-affine regime to distances greater than the lattice constant (or interatomic spacing) of the material. Experimental AFM spectra will generally cut off at a shorter wavenumber because of the finite radius of the probe tip, which limits the resolution. The normalization of the PSD given by Parseval's equation is preserved as long as $q_c\xi \gg 1$.

B. EMA model and fitting procedure

The optical properties of simulated surface roughness layers n_{EMA} (Sect. III.A.) are analyzed in terms of the isotropic Bruggeman EMA based on the optical constants of the bulk layer n_1 and a chosen value of f, here equal to 0.5[32]

$$f\,\frac{n_0^2 - n_{\mathrm{EMA}}^2}{n_0^2 + 2n_{\mathrm{EMA}}^2} + (1-f)\,\frac{n_1^2 - n_{\mathrm{EMA}}^2}{n_1^2 + 2n_{\mathrm{EMA}}^2} = 0. \tag{5}$$

The thickness d_s of the EMA layer is then extracted as the sole-fitting parameter using the goodness-of-fit function defined in the literature.[33] Fits are carried out both using commercial software for the acquisition and analysis of SE data (WASE and EASE from J. A. Woollam Co., Inc.) and our own software routine. Nearly identical values are obtained in all cases.

III. RESULTS

A. Model system: a-Si:H

The vapor-phase growth of a-Si:H has been extensively studied by real-time SE, so we consider this material as a model system. As mentioned in the Introduction, for growth on smooth substrates a linear relationship between w and d_s is often found.[16,21,24] (This does *not* include the morphologically complex stage of film nucleation and coalescence on a foreign substrate, where d_s rapidly increases then decreases, followed by the slow increase of d_s during steady-state film growth.)[34]

We begin by simulating the ellipsometric response of the a-Si:H surface as a function of the three parameters contained in the PSD, then transforming the output into the EMA roughness. The n_1 for a-Si:H is modeled using a well known Tauc-Lorentz model.[35,36] For various choices of α and ξ, thickness of the EMA layer increases with roughness but as w^2 rather than as w (Fig. 2), in apparent disagreement with experiment. When w and α (ξ) are held constant and ξ (α) is varied, the EMA thickness changes by a factor up to $\sim$3 (Fig. 2), again indicating the strong sensitivity of the EMA result to the details of the surface morphology. Similar variations are found if a value of f other than 0.5 is used.

Interestingly all the data presented in Fig. 2 coalesce into a single line when plotted as a function of a single-scaling parameter w^2/ξ^α. The resulting fit (Fig. 3) is $d_s = (3.5 \pm 0.1)\, w^2/\xi^\alpha + (0.37 \pm 0.05)$. Thus, *the parameter* w^2/ξ^α *contains all the relevant information that affects the scattering of light from a self-affine surface.*

An interpretation of this parameter can be obtained beginning with the average local slope of the surface $\delta = \langle(\nabla h)^2\rangle^{1/2}$. In the case of a self-affine surface, it can be shown that δ is proportional to w/ξ^α.[37] Thus, the measurement of EMA

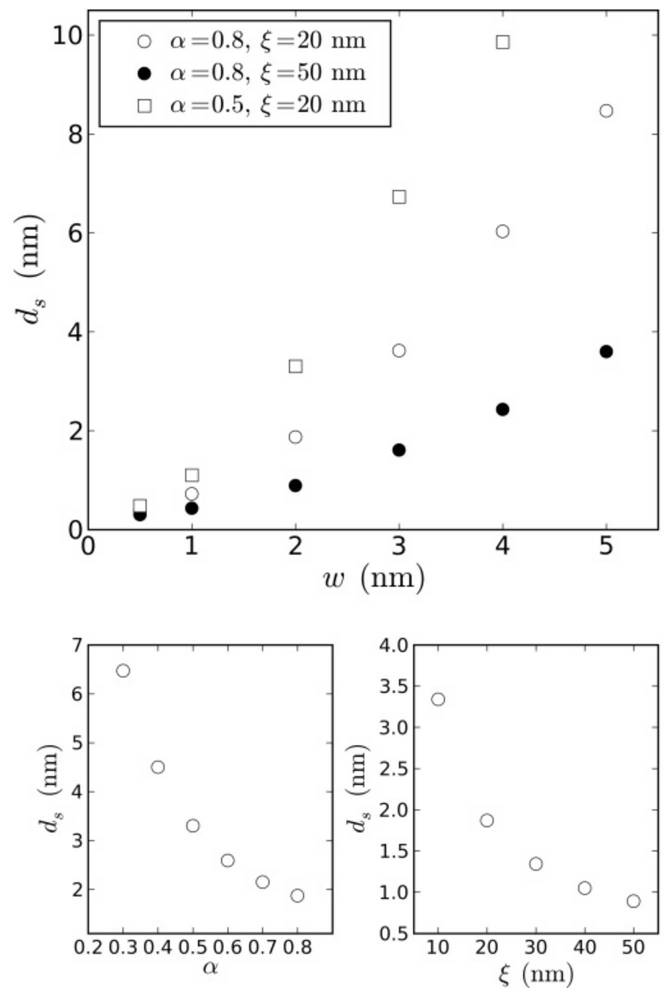

FIG. 2. Influence of surface roughness, roughness exponent, and correlation length on the thickness of the roughness layer for a-Si:H as obtained from the fitting of the Rayleigh-Rice scattering model.

roughness depends on the product $w\delta$. Each parameter offers information of a different nature: while w accounts for the interface width, i.e., characteristic vertical variations, δ is related to the waviness of the surface, i.e., the characteristic horizontal length over which the height variations occur. Interestingly the dependence of the optical properties on the $w\delta$ product is not limited to self-affine surfaces: Franta and Ohlídal observed the same dependence for (unphysical) model surfaces characterized by a Gaussian PSD, which have values of $\delta = \sqrt{2}w/\xi$ and yielded linear relationships between d_s/w and w/ξ.[29] Hence, they found $d_s \propto w^2/\xi$ for Gaussian PSDs, which again implies $d_s \propto w\delta$.

The scaling relationship between d_s and w^2/ξ^α automatically provides an explanation for the linear relationship found experimentally between the optical and rms roughness. The mechanisms leading to the formation of self-affine surfaces and the time evolution of the three parameters in the PSD have been amply studied.[1,19,38–40] Many systems undergo kinetic roughening that behaves according to dynamic-scaling theory. In these systems the long-scale roughness evolves with time as $w \sim t^\beta$, with β termed the growth exponent, whereas

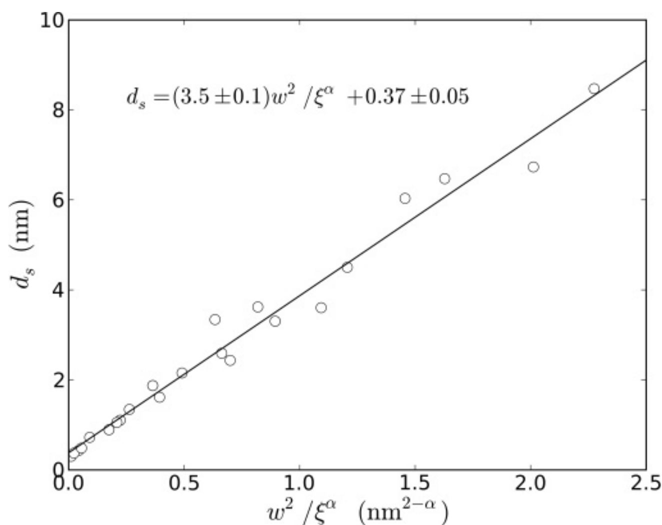

FIG. 3. Scaling of the thickness of the EMA roughness layer with the single parameter w^2/ξ^α for a-Si:H.

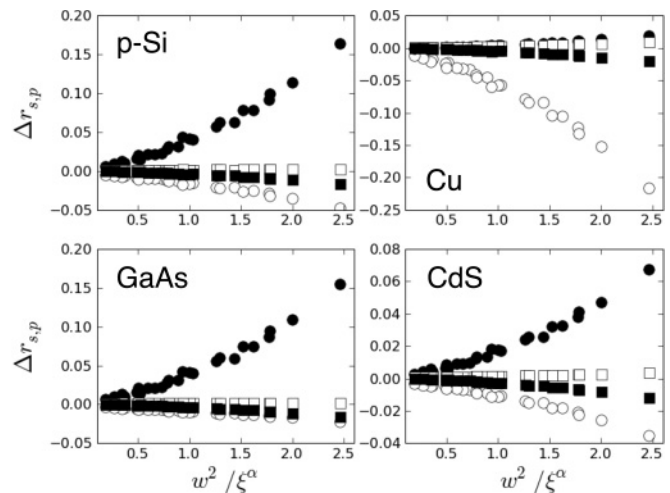

FIG. 4. Scaling of the real and imaginary parts of the Fresnel-reflection coefficient for the p (white circles, full circles) and s (white squares, full squares) polarizations with the parameter w^2/ξ^α for different materials obtained with the full Rayleigh-Rice scattering model ($\lambda = 500$ nm).

the correlation length changes as $\xi \sim t^{1/z} \sim t^{\beta/\alpha}$, where $z = \alpha/\beta$ is named the dynamic exponent. The exponents remain constant with time. A characteristic feature of such systems is that the average slope δ, which is proportional to w/ξ^α, does not change with time. Under this condition the change in the ellipsometric roughness becomes proportional to the change of the surface roughness, unlike the nonlinear predictions of Fig. 2. Provided that δ is approximately constant (changes only very slowly) during the growth of a-Si:H films, the linear correlation is now fundamentally understood. Differences in the coupling constant can therefore be attributed to differences in the local slope.

Explicit reports of the evolution of δ obtained from scanning probe microscopies are largely absent from the a-Si:H literature. However, plots of $S(q)$, the height-difference correlation function $H(r) = \langle[h(\mathbf{x}) - h(\mathbf{x}+\mathbf{r})]^2\rangle$, or w as a function of the lateral dimension of the measurement L provide some insight into how δ might change during deposition. If δ is constant (stationary growth), one would expect a series of $S(q)$ plots for various deposition times to overlap at high q. Similarly, plots of $H(r)$ or $w(L)$ should overlap for $r << \xi$ or $L << \xi$, respectively.[41] By examining the limited published data, we find some reports where a-Si:H film growth appears to be stationary.[9,42] In these cases our analysis shows that one should expect $d_s \propto w$. However, the proportionality constant between d_s and w would contain δ, so one would not expect a universal constant that applies to all deposition systems and all deposition conditions.

There are also reports where a-Si:H deposition appears to be nonstationary.[13,43,44] In other nonstationary film growth systems, the dynamic behavior of δ is often found to be relatively slow compared to w, and a logarithmic function is found: $\delta(t) \sim \sqrt{\ln t}$.[45] In this case d_s will become nearly proportional to w for long deposition times since the logarithmic function is much slower than $w \sim t^\beta$. In other cases a power law is found (anomalous scaling): $\delta(t) \sim t^\kappa$.[13,46] If this occurs, both early- and late-stage growth should yield $d_s \sim t^{\beta+\kappa}$. Therefore, using roughness data derived from ellipsometry to address detailed physical models (e.g., to obtain β)[7,9,11,14] requires extensive measurements of surface topology to examine δ and its dynamics.

B. Generalization to other materials

The scaling behavior obtained in Fig. 3 is an intrinsic feature of the nature of the scattering of rough surfaces and applies equally well to different materials. Solving Eq. (3) for a single wavelength and different values of surface roughness, correlation length, and roughness exponent, we confirm that the change in Fresnel coefficient also scales with w^2/ξ^α. This is true for any chosen wavelength. The change in the real and imaginary parts of the Fresnel reflection coefficients for p and s polarizations is calculated for poly-Si, GaN, CdS, and Cu using the Rayleigh-Rice scattering model of (1) (Fig. 4). Optical constants provided in Ref. 47 were used. The dependence on the single parameter w^2/ξ^α holds for all these materials. Consequently the scattering equation itself must contain the underlying reason for the results presented in the previous section.

To elucidate the nature of the scattering, we carried out an analytical approximation to the integral (1) in the limit where the wavelength of light is much larger than the surface correlation length $\lambda \gg \xi$. This limit is obeyed in high-quality thin-film surfaces. To first order in the $k_0\xi$ parameter, we have

$$S(q_x - n_0 k_0 \sin\theta_0, q_y) = S(q_x, q_y) \times \left[1 - 2(\alpha+1) n_0 \sin\theta_0 \frac{\xi q_x}{(1+\xi^2 q^2)^\alpha}(k_0\xi) + O(k_0\xi)^2\right]. \tag{6}$$

Because $q \gg k_0$ in most of the integration range of (1), we can use the asymptotic limit of the optical response functions $f_{p,s}$ given in (2) and (3). If

$$b = iq\left[1 - \frac{1}{2}\frac{n_0^2 k_0^2}{q^2} + O\left(\frac{k_0}{q}\right)^4\right]$$

and

$$c = iq\left[1 - \frac{1}{2}\frac{n_1^2 k_0^2}{q^2} + O\left(\frac{k_0}{q}\right)^4\right],$$

the reflection Fresnel coefficients can be written as

$$\Delta r_p = w^2 A_p + 2i\alpha w^2 \xi^{-2\alpha}\frac{n_0^2 - n_1^2}{n_0^2 + n_1^2} \times (B_{62p} - 2B_{31p})\int_0^{q_c}\frac{q^2 dq}{(q_\xi^2 + q^2)^{\alpha+1}} + 2\alpha w^2 \xi^{-2\alpha} k_0 \sin\theta_0 \frac{k_0^2 n_0^2 n_1^2 B_{61p} - B_{32p}k_0^{-2}}{n_0^2 + n_1^2} \quad (7)$$

and

$$\Delta r_s = w^2 A_s + 2i\alpha w^2 \xi^{-2\alpha}\frac{n_0^2 - n_1^2}{n_0^2 + n_1^2} B_{5s}\int_0^{q_c}\frac{q^2 dq}{(q_\xi^2 + q^2)^{\alpha+1}}, \quad (8)$$

where $q_\xi = 1/\xi$.

According to (7) and (8) the change in the Fresnel reflection coefficients is the sum of two contributions, one that depends only on the interface roughness (long-range roughness) and a second that also depends on the correlation length, roughness exponent, and the cutoff wavenumber (short-range features of the surface). The fact that in the full model the optical response scales with the parameter w^2/ξ^α indicates that the short-range contribution dominates with respect to the long-range one. This is consistent with previous experimental deductions that SE data are most sensitive to short-range roughness.[10,13,48]

The results of the full model (1) can be compared with the approximations given by (7) and (8); we consider realistic parameters $w = 2$ nm, $\xi = 20$ nm, $\alpha = 0.7$ and $q_c = 2\pi/0.2\ \mathrm{nm}^{-1}$, refraction indices $n_0 = 1$ and $n_1 = 2 + 2i$, and an angle of incidence of 70 degrees. Both approximations tend to the exact result in the long wavelength limit, and for $\lambda >$ 400 nm they provide good approximations to the more rigorous result (Fig. 5).

When the short-range terms in (7) and (8) become dominant, the optical- and surface-morphology contributions to $\Delta r_{p,s}$ can be separated, so that

$$\Delta r_{p,s} = C_{p,s}(n_0,n_1,k_0,\theta_0)F(w,\xi,\alpha,q_c), \quad (9)$$

where we have defined $F(w,\xi,\alpha,q_c)$ as

$$F(w,\xi,\alpha,q_c) = \alpha w^2 \xi^{-2\alpha}\int_0^{q_c}\frac{q^2}{(q_\xi^2 + q^2)^{\alpha+1}}dq \quad (10)$$

and

$$C_s(n_0,n_1,k_0,\theta_0) = 2i\frac{n_0^2 - n_1^2}{n_0^2 + n_1^2}B_{5s} \quad (11)$$

$$C_p(n_0,n_1,k_0,\theta_0) = 2i\frac{n_0^2 - n_1^2}{n_0^2 + n_1^2}(B_{62p} - 2B_{31p}). \quad (12)$$

When Eq. (9) holds, the scattering from self-affine surfaces is determined by $F(w,\xi,\alpha,q_c)$ regardless of the optical properties of the material. Thus, we obtain a universal behavior where the optical properties of the material only determine the amplitude of the perturbation of the Fresnel coefficients for a given self-affine surface.

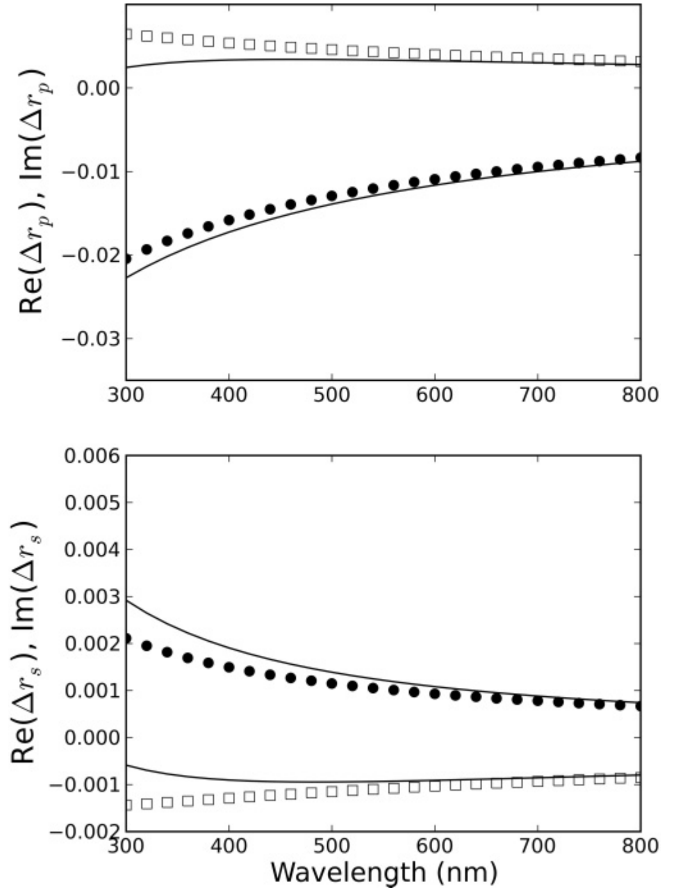

FIG. 5. Comparison between the real (full circles) and imaginary (open squares) part of the Rayleigh-Rice p and s Fresnel reflection coefficients and the analytic approximation given by (7) and (8) (full lines). See text for details.

We can further manipulate Eq. (10) to obtain a closed expression. After a change of variables, we obtain that

$$F(w,\xi,\alpha,q_c) = \frac{\alpha w^2}{2\xi}B\left(b;\frac{3}{2},\alpha - \frac{1}{2}\right), \quad (13)$$

where $B(x;n,m)$ is the incomplete Beta function and

$$b = \sqrt{\frac{(\xi q_c)^2}{1 + (\xi q_c)^2}}.$$

The dependence of F/w^2 with ξ and α, calculated from Eq. (13), is presented in Fig. 6 for $q_c = 2\pi/0.2\ \mathrm{nm}^{-1}$, ξ in the 10–50 nm range, and selected values of the roughness exponent α. When F/w^2 is plotted against the parameter α/ξ for different values of the roughness exponent, the curves do not coalesce to a single plot (Fig. 6, top). However, when plotted against the scaling parameter $\xi^{-\alpha}$, the curves coalesce to a single trend (Fig. 6, bottom).

The influence of the cut-off parameter q_c is negligible as long as $\xi q_c \gg 1$. In this case $b \to 1$ and $\lim_{b\to 1} B(b;\frac{3}{2},\alpha - \frac{1}{2}) = B(\frac{3}{2},\alpha - \frac{1}{2})$. This is only possible for $\alpha \geqslant 0.5$ because the incomplete Beta function does not converge to a finite value for $\alpha < 0.5$. Under these conditions

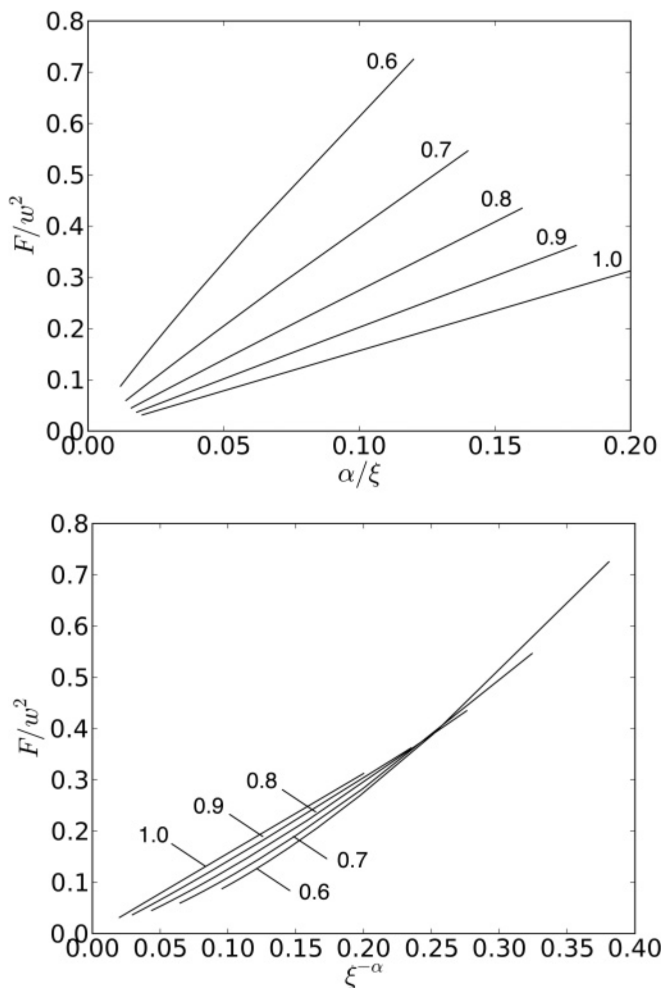

FIG. 6. Scaling of the function F with the single parameter w^2/ξ^α.

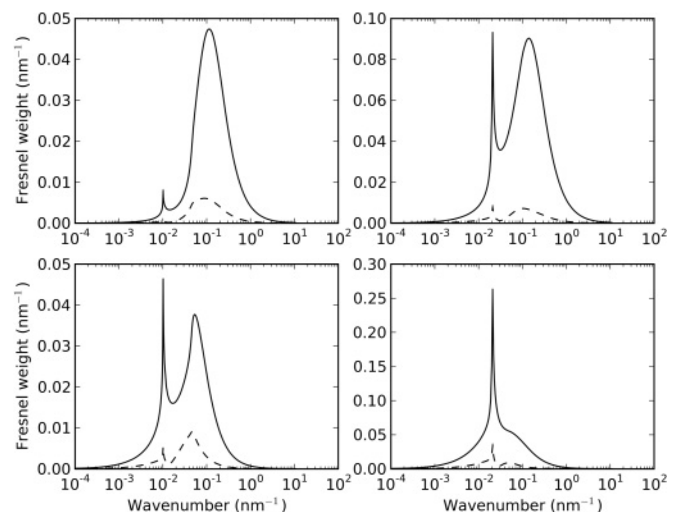

FIG. 7. Surface wavenumber influence on the Rayleigh-Rice scattering of an a-Si:H self-affine surface ($w = 2$ nm, $\alpha = 0.8$) for p (full line) and s (dashed line) polarizations. Top left: $\xi = 10$ nm, $\lambda = 620$ nm; top right: $\xi = 10$ nm, $\lambda = 310$ nm; bottom left: $\xi = 30$ nm, $\lambda = 620$ nm; bottom right: $\xi = 30$ nm, $\lambda = 310$ nm.

the contributions of wavenumbers close to the cutoff cannot be neglected and the scaling behavior breaks down. The influence of $\xi q_c \gg 1$ in the scaling behavior can be demonstrated for $\alpha = 1$. In this case the integral in Eq. (10) has an analytic solution and, assuming $\xi q_c \gg 1$, $F(w,\xi,\alpha,q_c) = \frac{w^2}{2\xi} B(\frac{3}{2},\frac{1}{2}) \sim w\delta$. This result is consistent with the general scaling behavior proposed in the previous section and the same as that obtained in the Gaussian case, differing only on the magnitude of the proportionality constant. If the condition $\xi q_c \gg 1$ does not hold, the $F \sim w\delta$ scaling breaks down.

Finally, from Eq. (13) it is possible to determine the sensitivity of light scattering to the variation of each surface parameter. For a surface roughness of 2 nm, correlation length of 10 nm, and roughness exponent α of 0.8, a 10% variation in w, ξ, or α separately causes a change in F of 20%, 7%, and 10%, respectively.

C. Limits of the scaling behavior: Influence of the correlation length

The two requirements for the Rayleigh-Rice theory to be a good approximation of the scattering process are that both surface roughness and correlation length must be smaller than the light wavelength. Moreover, a necessary condition for the dependence with w^2/ξ^α is that the high-wavenumber contribution to the integral of the scattering equations must be dominant. Otherwise, the ellipsometric response would be independent of the structure of the PSD at high wavenumbers.

In Fig. 7 we present the calculated contribution of each wavenumber to the optical response of the surface for four different conditions. When the correlation length is much smaller than the wavelength of the light, the most important contributions are from wavenumbers of the order of the correlation length. Under this condition the scaling behavior of Figs. 3 and 4 is fulfilled. When the correlation length is comparable to the wavelength, the contribution of the long wavenumbers decreases, and a secondary contribution (peak) appears at a wavenumber corresponding to that of the incident radiation. This additional contribution is a consequence of a resonance in the kernel of the scattering equations of the Rayleigh-Rice model. Both the results presented in Fig. 7 and the breakdown of the analytic approximation derived in the previous section at low wavelengths indicate that the scaling behavior depicted in Figs. 3 and 4 holds whenever the correlation length is shorter than the wavelength of the light, a situation that is often found in high quality thin film systems. Because the Rayleigh-Rice approximation is no longer correct as $\xi \to \lambda$, it is very difficult to ascertain whether the breakdown of the scaling behavior and the resonance depicted in Fig. 7 have a physical origin or are an artifact of the theory as the correlation length approaches the wavelength of the incident radiation.

IV. CONCLUSIONS

We have studied the influence of surface morphology on the optical response of self-affine surfaces, in particular, how the parameters of correlation length ξ and roughness exponent α affect the thickness of the EMA surface-roughness layer obtained using SE. In general, optical theory predicts that the EMA roughness should not be a linear function of the

rms roughness extracted from AFM measurements. However, we show that when the average surface slope δ changes only slowly with film thickness, then a linear relationship is restored. We further show that this result holds independent of the optical properties of the surface in question. These results rationalize the apparently inconsistent results in the literature for surface roughness of a-Si:H: differences between studies can be interpreted in terms of differences in the local slope of the roughness.

ACKNOWLEDGMENTS

The authors gratefully acknowledge support by the University of Illinois Campus Research Board (B.A.S.) and by the Fundacion la Caixa and the Spanish MEC/FECYT (A.Y.-G.).

APPENDIX

In this section we include the definitions of the A_i, B_i coefficients in the $f_{p,s}(q_x,q_y)$ kernels defined in (2) and (3). They only depend on the optical properties of the interface media, the wavelength, and the incident angle:

$$\begin{aligned}
A_p &= k_0^2 n_0 n_1^2 X/D \\
B_{31p} &= k_0 n_0^2 n_1^2 \sin\theta_0 W/D \\
B_{32p} &= k_0^3 n_0^2 n_1^2 \sin\theta_0 X/D \\
B_{61p} &= n_0 n_1 \cos\theta_1 W/(k_0 D) \\
B_{62p} &= k_0 n_0 n_1 \cos\theta_1 X/D \\
A_s &= -2k_0^2 n_1 \cos\theta_1 n_0 \cos\theta_0 r_s^0 \\
B_{5s} &= -2k_0 n_0 \cos\theta_0 r_s^0,
\end{aligned}$$

where

$$D = (n_0\cos\theta_0 + n_1\cos\theta_1)\left(n_0^2\sin^2\theta_0 + n_0\cos\theta_0 n_1\cos\theta_1\right)$$

$$X = \left(n_0^2 - n_1^2\right)\cos\theta_1 t_p^0$$

$$W = \left(n_1^2/n_0^2 - 1/n_1\right) n_0 \sin\theta_0 t_p^0$$

and r_s^0 and t_p^0 are the Fresnel reflection and transmission coefficients for the s and p polarizations, and θ_1 is defined from the complex Snell's law $n_0\sin\theta_0 = n_1\sin\theta_1$.

---

[*]Present address: Argonne National Laboratory, Argonne, Illinois 60439, USA.

[†]Present address: National Institute of Standards and Technology, Gaithersburg, Maryland 20899, USA.

[‡]Corresponding author: abelson@illinois.edu

[1] A.-L. Barabási and H. E. Stanley, *Fractal Concepts in Surface Growth* (Cambridge University Press, Cambridge, UK, 1995), p. 23.

[2] D. G. Cahill, J. Vac. Sci. Technol. A **21**, S110 (2003).

[3] A. Mazor, D. J. Srolovitz, P. S. Hagan, and B. G. Bukiet, Phys. Rev. Lett. **60**, 424 (1988).

[4] R. P. U. Karunasiri, R. Bruinsma, and J. Rudnick, Phys. Rev. Lett. **62**, 788 (1989).

[5] V. K. Singh and E. S. G. Shaqfeh, J. Vac. Sci. Technol. A **11**, 557 (1993).

[6] G. S. Bales and A. Zangwill, J. Vac. Sci. Technol. A **9**, 145 (1991).

[7] A. H. M. Smets, D. C. Schram, and M. C. M. van de Sanden, J. Appl. Phys. **88**, 6388 (2000).

[8] D. H. Levi, B. P. Nelson, J. D. Perkins, and H. R. Moutinho, J. Vac. Sci. Technol. A **21**, 1545 (2003).

[9] A. H. M. Smets, W. M. M. Kessels, and M. C. M. van de Sanden, Appl. Phys. Lett. **82**, 865 (2003).

[10] B. A. Sperling and J. R. Abelson, Appl. Phys. Lett. **85**, 3456 (2004).

[11] W. M. M. Kessels, J. P. M. Hoefnagels, E. Langereis, and M. C. M. van de Sanden, Thin Solid Films **501**, 88 (2006).

[12] I.-Y. Kim, S.-H. Hong, A. Consoli, J. Benedikt, and A. von Keudell, J. Appl. Phys. **100**, (2006).

[13] B. A. Sperling and J. R. Abelson, J. Appl. Phys. **101**, 024915 (2007).

[14] M. A. Wank, R. A. C. M. M. van Swaaij, and M. C. M. van de Sanden, Appl. Phys. Lett. **95**, 021503 (2009).

[15] D. E. Aspnes and J. B. Theeten, Phys. Rev. B **20**, 3292 (1979).

[16] H. Fujiwara, J. Koh, P. I. Rovira, and R. W. Collins, Phys. Rev. B **61**, 10832 (2000).

[17] S. G. Mayr, M. Moske, and K. Samwer, Phys. Rev. B **60**, 16950 (1999).

[18] T. Karabacak, Y. P. Zhao, G.-C. Wang, and T.-M. Lu, Phys. Rev. B **66**, 075329 (2002).

[19] F. Ojeda, R. Cuerno, R. Salvarezza, F. Agulló-Rueda, and L. Vázquez, Phys. Rev. B **67**, 245416 (2003).

[20] A. Yanguas-Gil, J. Cotrino, A. Walkiewicz-Pietrzykowska, and A. R. González-Elipe, Phys. Rev. B **76**, 075314 (2007).

[21] J. Koh, Y. W. Lu, C. R. Wronski, Y. L. Kuang, R. W. Collins, T. T. Tsong, and Y. E. Strausser, Appl. Phys. Lett. **69**, 1297 (1996).

[22] P. Petrik, L. P. Biró, M. Fried, T. Lohner, R. Berger, C. Schneider, J. Gyulai, and H. Ryssel, Thin Solid Films **315**, 186 (1998).

[23] P. Petrik, T. Lohner, M. Fried, L. P. Biró, N. Q. Khánh, J. Gyulai, W. Lehnert, C. Schneider, and H. Ryssel, J. Appl. Phys. **87**, 1734 (2000).

[24] H. Fujiwara, M. Kondo, and A. Matsuda, Phys. Rev. B **63**, 115306 (2001).

[25] A. A. E. Stevens and H. C. W. Beijerinck, J. Vac. Sci. Technol. A **23**, 126 (2005).

[26] J. Isidorsson, C. G. Granqvist, K. von Rottkay, and M. Rubin, Appl. Opt. **37**, 7334 (1998).

[27] B. A. Sperling, Ph.D. dissertation, University of Illinois at Urbana-Champaign, 2006.

[28] D. Franta and I. Ohlídal, J. Mod. Opt. **45**, 903 (1998).

[29] D. Franta and I. Ohlídal, Opt. Commun. **248**, 459 (2005).

[30] G. Palasantzas, Phys. Rev. B **48**, 14472 (1993).

[31] G. Palasantzas, Phys. Rev. B **49**, 5785 (1994).

[32] D. E. Aspnes, Thin Solid Films **89**, 249 (1982).

[33] G. E. Jellison Jr., in *Handbook of Ellipsometry*, edited by H. G. Tompkins and E. A. Irene (Springer-Verlag, Heidelberg, Germany and William Andrew Publishing, Norwich, NY, 2005), pp. 268–271.

[34] Y.-M. Li, I. An, H. V. Nguyen, C. R. Wronski, and R. W. Collins, Phys. Rev. Lett. **68**, 2814 (1992).

[35] G. E. Jellison and F. A. Modine, Appl. Phys. Lett. **69**, 371 (1996).

[36]G. E. Jellison and F. A. Modine, Appl. Phys. Lett. **69**, 2137 (1996).
[37]G. Palasantzas, Phys. Rev. E **56**, 1254 (1997).
[38]F. Ojeda, R. Cuerno, R. Salvarezza, and L. Vázquez, Phys. Rev. Lett. **84**, 3125 (2000).
[39]W. M. Tong and R. S. Williams, Annu. Rev. Phys. Chem. **45**, 401 (1994).
[40]M. Pelliccione and T.-M. Lu, *Evolution of Thin Film Morphology: Modeling and Simulations* (Springer-Verlag, Berlin, 2008), pp. 29–46, 61–78, 93–144.
[41]T. Karabacak, Y. P. Zhao, G.-C. Wang, and T.-M. Lu, Phys. Rev. B **64**, 085323 (2001).
[42]D. M. Tanenbaum, A. L. Laracuente, and A. Gallagher, Phys. Rev. B **56**, 4243 (1997).
[43]G. T. Dalakos, J. L. Plawsky, and P. D. Persans, Appl. Phys. Lett. **85**, 3462 (2004).
[44]K. R. Bray and G. N. Parsons, Phys. Rev. B **65**, 035311 (2002).
[45]J. H. Jeffries, J. K. Zuo, and M. M. Craig, Phys. Rev. Lett. **76**, 4931 (1996).
[46]J. M. López, Phys. Rev. Lett. **83**, 4594 (1999).
[47]J. A. Woollam Co., EASE Software (included data files).
[48]C. Pickering, R. Greef, and A. M. Hodge, Semicond. Sci. Technol. **4**, 574 (1989).